Hindawi
International Journal of Aerospace Engineering
Volume 2021, Article ID 4652556, 16 pages
https://doi.org/10.1155/2021/4652556

Research Article

Finite Element Simulations of Dynamic Shear Fracture of Hollow Shear Pins

Zibo Jin,[1] **Jin Zhou**,[1,2] **and Daochun Li**[1]

[1]*School of Aeronautic Science and Engineering, Beihang University, Beijing 100000, China*
[2]*Chinese Aeronautical Establishment, Beijing 100012, China*

Correspondence should be addressed to Jin Zhou; zhoujin@buaa.edu.cn

Received 2 May 2021; Revised 3 August 2021; Accepted 26 August 2021; Published 23 September 2021

Academic Editor: Teng Wu

The shear pin structure is widely used in aeronautics and astronautics structures to deal with emergency structure separation problems. The shear pin design has a strict restriction on the precise failure load and definite failure mode. Previous research has conducted shear fracture tests and simulations of solid shear pins while there is a lack of detailed research on the shear fracture of hollow shear pins with large diameters. In this research, a 3-dimensional finite element model was built based on the actual shear pin installed on the aircraft engine pylon and the model was validated by the experiment. The influences of the inner diameter of hollow shear pins on the shear fracture process were investigated by conducting finite element simulations. The structural deformation, energy dissipation in the fracture process, and failure load of shear pins were evaluated. It is found that as the inner diameter increases, the failure mode of shear pins changed and would result in difficulties on the structure separation. To solve this problem, a new configuration of hollow shear pin was proposed for the purpose of obtaining both desired failure load and failure mode. The new configuration was verified by the fracture simulation and it is found that the new configuration is effective and can be used to improve the shear fracture performance.

1. Introduction

The shear pin is a mechanical sacrificial component like an electric fuse designed to break itself when it arises the mechanical overload to prevent the severe damage of the global structure [1]. The shear pin structures can be applied to the crashworthy design realization that is widely used in aeronautics and astronautics structures to deal with emergency structure separation problems. During the emergency landing of aircraft, the engine pylon is easy to puncture or tear the fuel tank, resulting in fuel leakage, catastrophic fire, and even explosion. The pylon emergency breaking-away techniques through controlling fracture sequence of shear pins can be effective ways to protect passengers from fire and explosions caused by wing tank damage [2, 3]. The shear pins are also used in landing gear to collapse in a controlled manner so that the landing gear does not penetrate the cabin and cause secondary hazards when faced with urgent situations [4–6]. The shear pin of wind turbine generators is generally designed in such a way that it should fail when the mechanical overloads come up so as to protect the highly expensive units, namely, the gearbox and the generator [1]. Another case is the rocket's shear pin used in caging and protection mechanism of missile launchers, whose main function is locking the missile in launching shoe when launch force is smaller than release force and then cut off quickly to relieve the constraint when launching force reaches release force [7]. Similar structure separation mechanisms are also found in spacecraft such as satellites [8].

From the safety and design point of view, the most important factor of shear pins is the reproducibility and the repetitiveness of failure load and failure mode. Moreover, in case of multiple failures, the sequence of failures shall be assured. Therefore, the shear pin design has a strict restriction on the precise fracture load and definite failure mode. Too large failure load will make the shear pin unable to break as required and cause separation failure while too small failure load will result in the loss of safety factors.

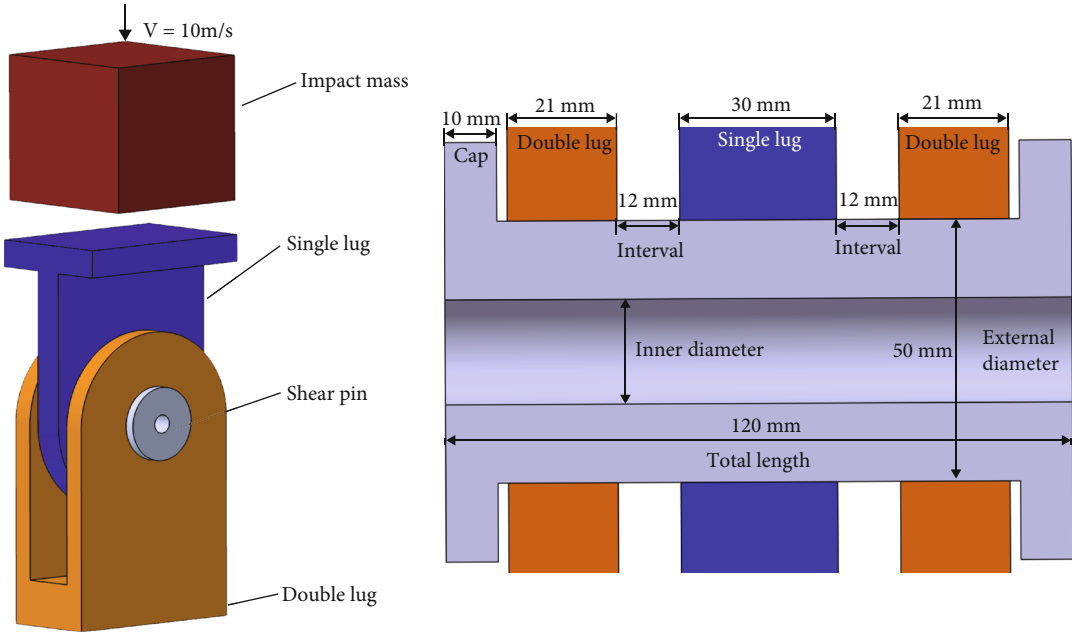

Figure 1: Geometry parameters of the shear pin and its connecting lugs.

Table 1: Material properties.

Materials	Mass density	Materials	Mass density
15-5PH stainless steel	$7.78E-9$	195000	0.28
TC4	$4.51E-9$	110000	0.34

Table 2: Johnson–Cook model parameters for 15-5PH.

A (MPa)	B (MPa)	n	C	m
855	448	0.14	0.0137	0.63

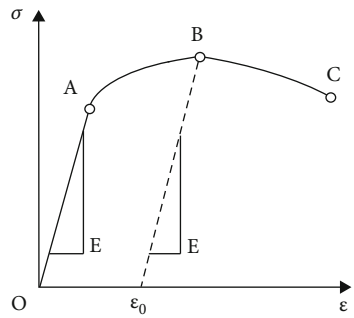

Figure 2: Characteristic stress-strain behaviour of the 15-5PH stainless steel.

The failure mode of shear pins should be simple and clear to ensure that the structure can be separated without getting stuck.

Previous researchers performed experimental and numerical investigations to quantify the failure load and fracture process of shear pin structures. Peng [9] conducted shear fracture tests of shear pins and established a bilinear model. Relevant research suggests that ultimate deformation and equivalent stiffness of the equivalent linear model are approximately proportional to the diameter of the shear pin, and load capability is approximately proportional to the square of the diameter of the shear pin [10]. Sankar et al. investigated the failure mechanism by both visual and scanning electron microscope (SEM) inspection on the fractured surface and optimized the neck diameter of shear pin for the safe operation [1]. Antoni [11] studied the contact nonlinearities of shear pin structures through an analytical contact model and finite element analysis. The failure behaviours and fracture performance of similar double-shear structures were studied [12]. The mechanical analysis of the connecting structures of shear pins was also carried out through theoretical analysis and numerical simulation [13, 14].

Most of the shear fracture tests and simulations of shear pins mentioned above mainly focused on the solid pins or pins with small diameters. For the shear pins with large diameters installed in large component such as aircraft engine pylon, solid configuration design will make the failure load too high and hard to fracture, causing difficulties in the structure separation process. Therefore, the shear pins with large diameters adopt hollow structural configuration to reduce failure load [2]. The failure load and failure mode of hollow shear pin are more complicated than the solid pin and are greatly affected by the inner diameters. Dong [15] conducted shear fracture tests and numerical simulations on shear pins of specific configurations that installed in the engine pylon. There is still a lack of detailed research on the shear fracture of hollow shear pins.

Another problem should be considered is that the pin structures with large inner diameters tend to generate large plastic deformations in the fracture process, which is similar

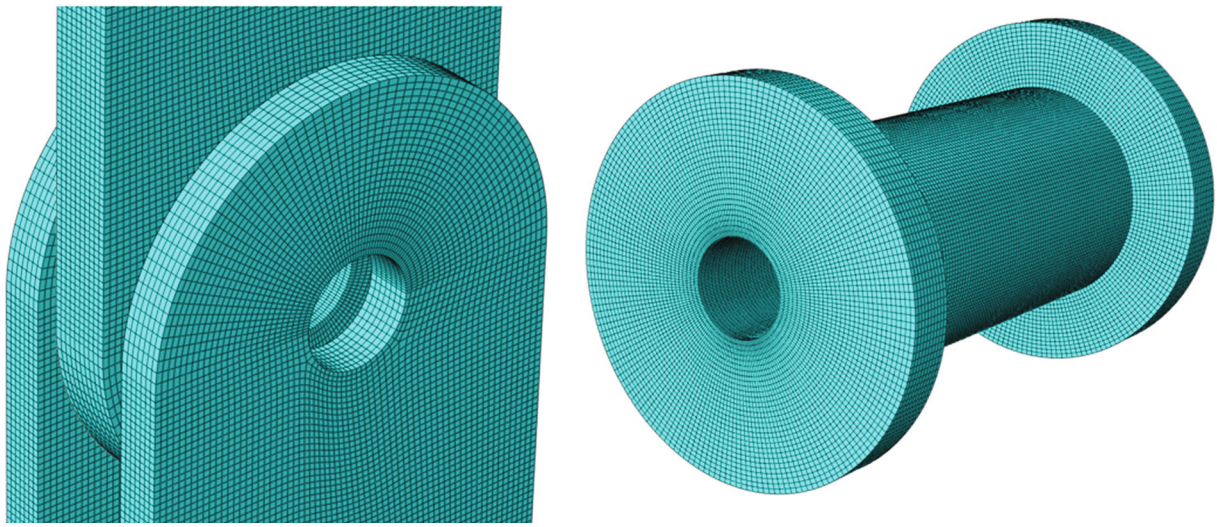

Figure 3: Mesh of the shear pin and its connecting lugs.

with the fracture process of the tube structures [16–18]. The large plastic deformation of shear pins may cause difficulties in structural separation process. Boeing has presented some structural configurations for hollow shear pins to improve shear fracture performance, but it has not been sufficiently verified.

In this research, the shear fracture process and failure mode of hollow shear pin were studied. With reference to the shear pin structure installed on the aircraft engine pylon, a 3-dimensional finite element model was build based on the geometry parameters, structural configuration, and materials of the actual shear pin of engine pylon. The fracture process of the shear pin was simulated using the finite element model, and the results were validated by the experiment. The influence of inner diameter on the shear pin was investigated by conducting fracture simulations of shear pins with different inner diameters. The structural deformation and stress distribution during the fracture process, failure load, and energy dissipation were evaluated. To solve the problem that the shear pins with large inner diameters would generate large plastic deformation and cause separation difficulties, a new inner-varying configuration of hollow shear pin was proposed. The new configuration provides a solution for changing the failure mode of shear pin without changing the external shape of shear pins. The fracture simulations of the new configuration were examined, and the influence of the geometry parameters on the failure mode, failure load, and energy dissipation was studied.

2. Materials and Methods

2.1. Geometry and Structure. The shear pin structure studied in this research refers to the shear pin installed on the civil aircraft engine pylon whose function is to break away aircraft engine and to prevent fuel tank damage and fire in the aircraft emergency landing [2, 3]. The shear pin can be thought of as a hollow cylinder with two end caps. The shear pin is fixed by a single lug and a double lug. The geometry parameters of the shear pin are based on the actual shear pin structure of engine pylon [3]. The external diameter of the actual shear pin ranges from 40 mm to 56 mm. In this research, the external diameter was set as 50 and the inner diameter ranged from 16 to 32 mm which was selected to study the influence of change of inner diameters on the shear fracture of shear pins. The total length of the shear pin was 110 mm, and the thickness of each end cap was 10 mm. The thickness of the lugs and the intervals between lugs were determined with reference to the actual shear pin configuration of engine pylon [3, 15]. The geometry parameters of the shear pin and its connecting lugs are shown in Figure 1.

The fracture simulation method of shear pins was through striking an impact mass against the single lug of the double shear structure, as shown in Figure 1. The double lug bottom was fixed to the ground to provide support force. The impact velocity needs to comply with the loading velocity in the actual engineering application and working conditions. The shear pin of the engine pylon of civil aircraft is designed to fracture in emergency landing conditions of aircrafts. Therefore, the impact velocity of emergency landing conditions was used in the fracture simulations. Based on the actual aircraft crash events, airworthiness regulations, and previous aircraft structure impact crash experiments, the impact velocity was set as 10 m/s [2].

2.2. Material and Damage Model. The materials of the shear pin and the connecting lugs are 15-5PH stainless steel and titanium alloy Ti6-Al4-V, respectively, according to the actual shear pin structure of the engine pylon. Both 15-5PH and Ti6-Al4-V have isotropic elastic properties defined in Table 1. A Johnson–Cook stress model has been used to model the plastic properties. The Johnson–Cook model is expressed as follows:

$$\sigma = (A + B\varepsilon^{n})(1 + C\ \ln \dot{\varepsilon}^{*})(1 - T^{*m}), \quad (1)$$

where σ is flow stress in MPa, ε is the true strain, $\dot{\varepsilon}^{*}$ is the dimensionless strain rate, A (MPa) is the yield strength, B (MPa) is the hardening modulus, C is the strain rate

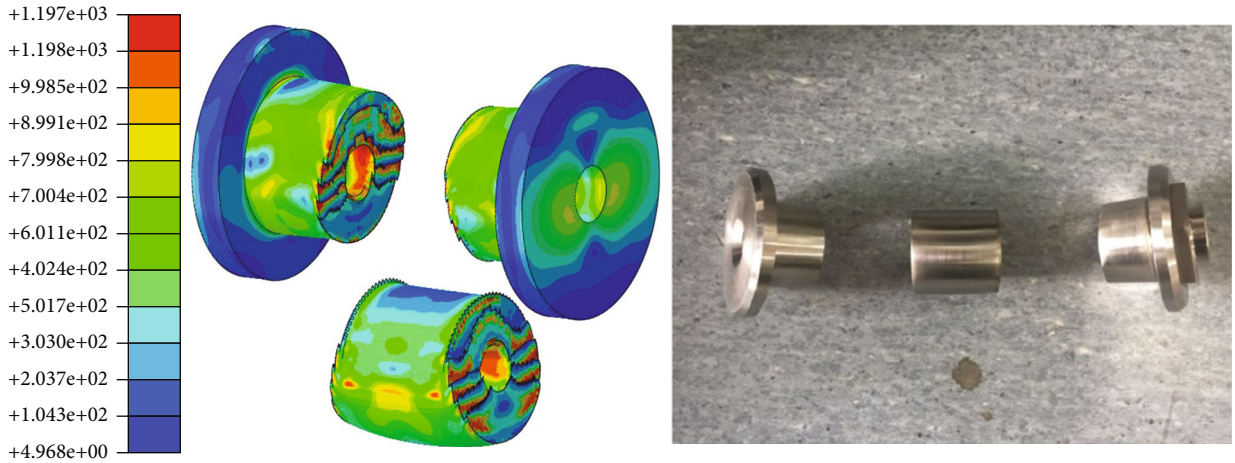

(a) Shear pin with inner/external diameter ratio of 0.38

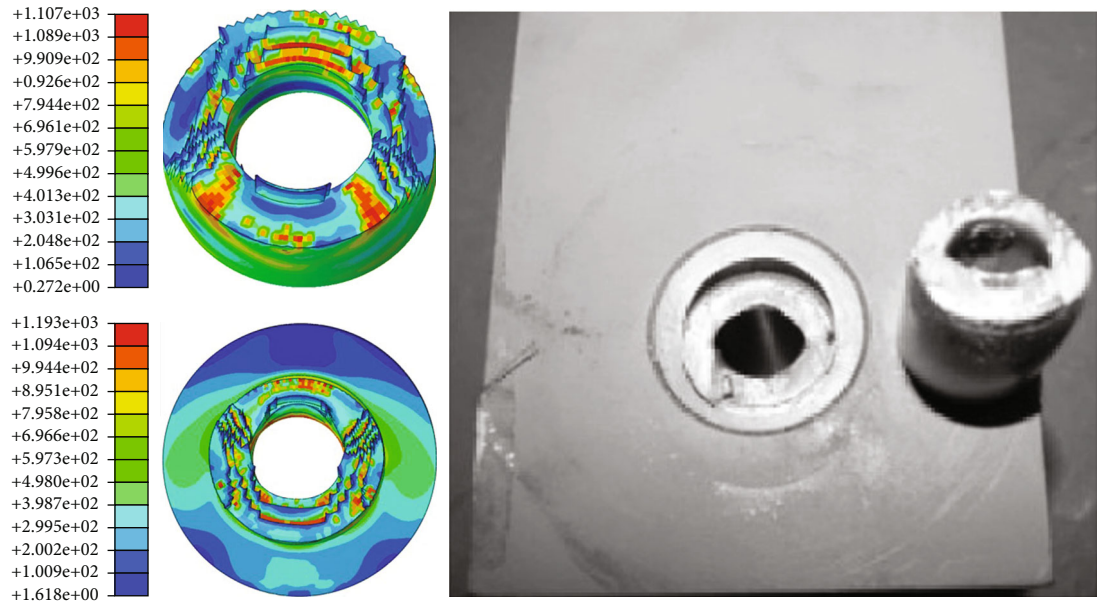

(b) Shear pin with inner/external diameter ratio of 0.56

Figure 4: Comparison of simulation results and test results.

sensitivity coefficient, n is the hardening coefficient, and m is the thermal softening coefficient. The Johnson–Cook model describes the dynamic characteristics of strain rate hardening, strain hardening, and thermal softening of metal materials. The Johnson–Cook model parameters are presented in Table 2. The model parameters are obtained by the specimen impact tests [19, 20]. Considering the requirements of test loading rate, the impact tests are mainly tensile tests, but the Johnson–Cook model has also been used in shear simulations and achieved good results.

The shear pins experience large deformation and damage in the fracture process. In order to accurately simulate the fracture process of the pin structure, it is necessary to establish a reasonable and effective damage model. Figure 2 illustrates the characteristic stress-strain behaviour of the 15-5PH stainless steel undergoing damage. The stress-strain diagram shows a clear division of stages. The initial stage of material deformation is linear elastic deformation (section O-A), and then, with the strengthening of strain, the material enters the plastic yield stage (section A-B). After exceeding point B, the bearing capacity of the material decreases significantly until fracture (B-C section). Point B indicates the beginning of material damage, also known as the standard of damage beginning. Beyond this point, the stress-strain curve is determined by the progress of stiffness weakening in the local deformation region.

Based on the stress-strain behaviour of the 15-5PH, the ABAQUS ductile damage model was used to simulate the damage evolution. The damage model includes the softening of the yield stress and degradation of the elasticity as shown in Figure 2. The equivalent plastic strain ε_0 was set as 0.1 according to the specimen tensile experiments [15], which indicates the beginning of the material damage. The material failure is caused by the complete loss of material bearing

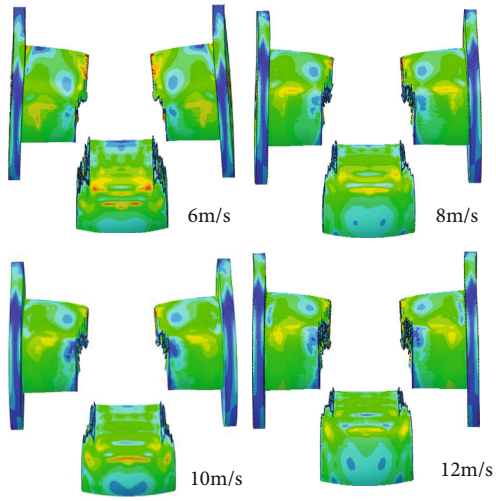

Figure 5: Final failure modes of shear pins of different loading rates.

capacity. The displacement damage evolution was used to define the material failure. Elements deforming past displacement limit are removed from the simulations, resulting in gap openings in the structures, which can be considered to behave similarly to the cracks developing in the shear pins. The displacement limit can be obtained by the product of the meshing characteristic length and equivalent failure strain. The equivalent failure strain can refer to the specimen tensile experiments and material elongations. The elongation of 15-5PH stainless steel varies from 12% to 25% according to different heat treatment methods and forming methods [15, 21, 22]. In this research, the displacement limit was set according to the references and the model validation.

2.3. Finite Element Model. A full-scale 3-dimensional finite element model of the shear pin structure was developed using the explicit, nonlinear 3D finite element code. The accumulation errors of finite element simulations generally result from too many assumptions and approximations made based on oversimplified finite element models. Therefore, the geometry of the model must confirm the actual model, and the discretization process must reflect the original structural behaviours through proper element formulations. The hexahedral solid elements were used to model the shear pin and supporting lugs. The mesh density of the shear pin and the lug was 1 mm and 3 mm, respectively, and the finite element model was discretized as 624458 nodes and 987720 elements, as shown in Figure 3. The solid elements employed a reduced-integration scheme in calculating element stiffness to enhance solution efficiency.

Considering the contact that may occur during fracture process of the shear pin structure, all shear pin nodes were defined a node to surface with the lugs to ensure the effective contact between shear pin and lugs. A self-contact of the shear pin was defined to calculate the internal contact of the shear pin after pin fracture. The friction coefficients in the contact interfaces were assumed 0.2, and a "hard-contact" algorithm was adopted. The final model was performed with the explicit solver ABAQUS/Explicit.

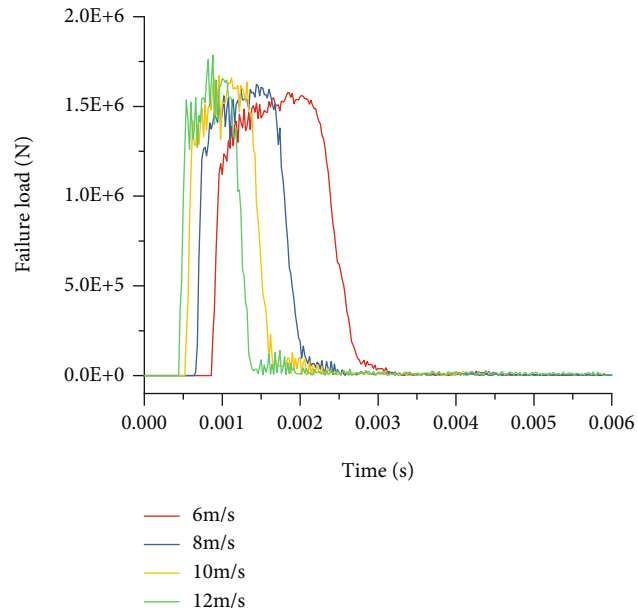

Figure 6: Contact force between shear pins and its connecting lugs.

2.4. Model Validation. The finite element model built in this research was validated by the shear fracture test of shear pins using the same materials and structural configuration [15, 23]. The diameters of the shear pin of the simulation are slightly different from those of the tests, but the ratio of the inner diameter to the external diameter was kept consistent. Moreover, the intervals between lugs are important factors to the shear fracture process, which was set the same as that of the tests.

Dong [15] conducted the fracture test of the shear pin with the inner diameter of 16.95 mm and the inner diameter/external diameter ratio of 0.38, as shown in Figure 4(a). The pin structure was subjected to shear load and cut into three pieces. The fracture surface is relatively flat and perpendicular to the pin axis. Li et al. [23] studied the shear strength of shear pin with the inner diameter of 12.4 mm and the inner diameter/external diameter ratio of 0.56, as shown in Figure 4(b). It can be seen through the broken pieces that the shear pin generated obvious plastic deformation and the fracture surface is inclined.

It should be mentioned that the fracture tests were carried out under static loading, the effect of loading rate is not included, and the load-deformation response is difficult to collate with the impact-loading simulations. For mental materials, the load resistance generally increases with the increasing loading rate. To verify the effects of the loading rate on the fracture process of the shear pins and the effectiveness of the Johnson–Cook models, the shear fracture of pin structures with different loading rates was carried out. In the dynamic fracture simulations, the loading rate was determined through changing the impact velocity of the impact mass. The impact velocities of 6 m/s, 8 m/s, 10 m/s, and 12 m/s were selected, and the simulation results are shown in Figure 5. The structural deformations and failure modes of shear pins are basically consistent, which demonstrates that the loading rate has little influence on the failure

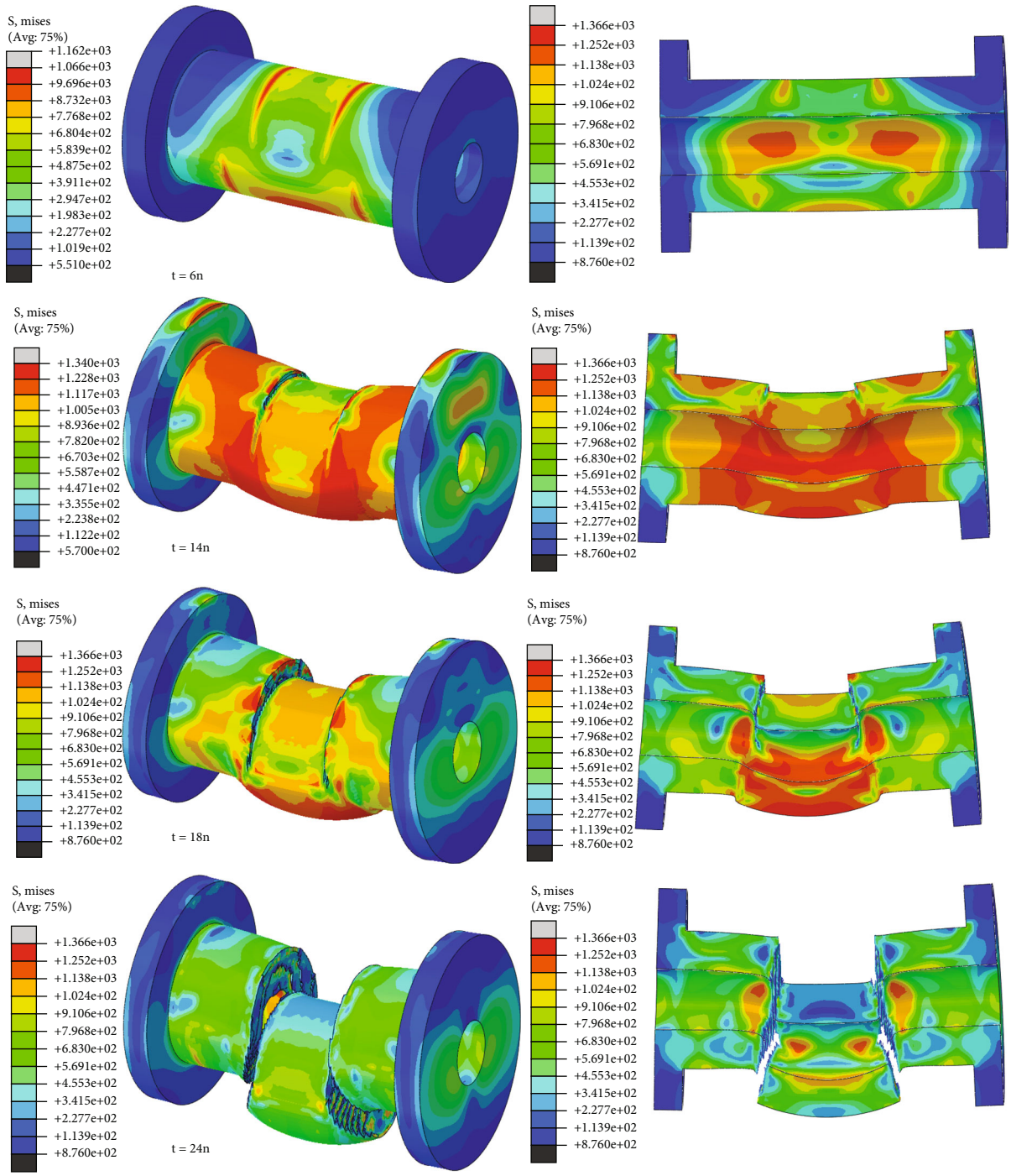

(a) Inner diameter of 22 mm

Figure 7: Continued.

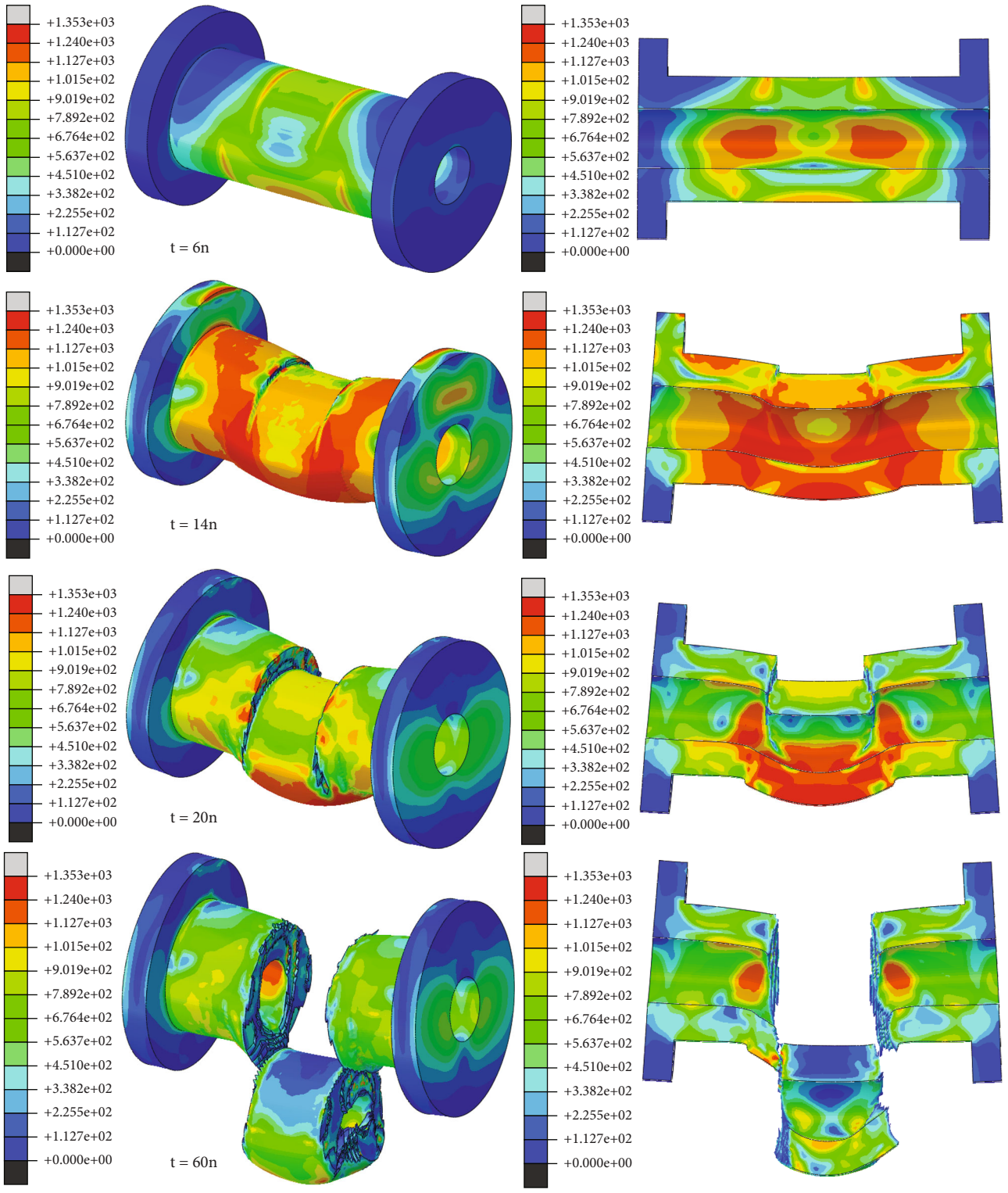

(b) Inner diameter of 24 mm

Figure 7: Continued.

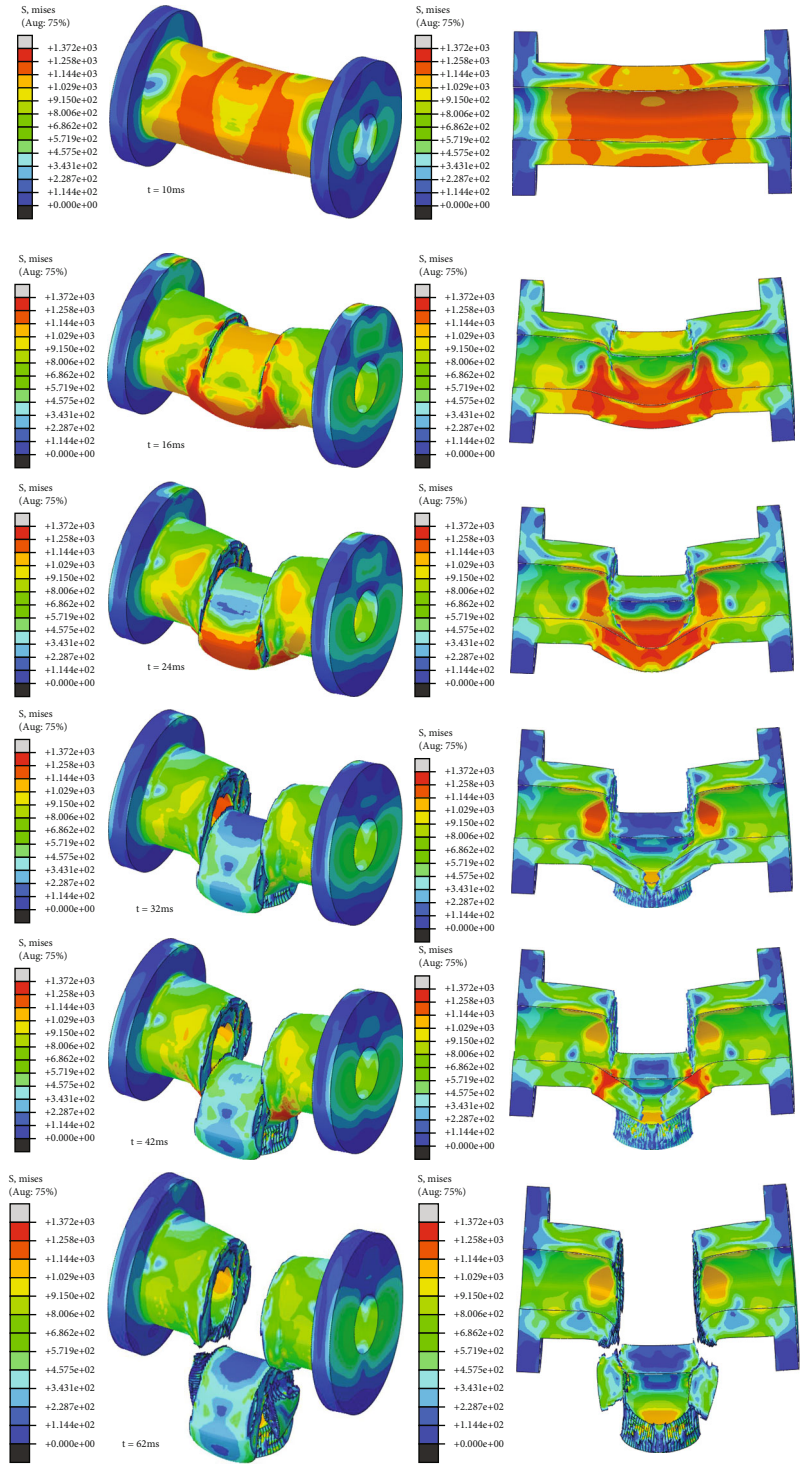

(c) Inner diameter of 26 mm

Figure 7: Continued.

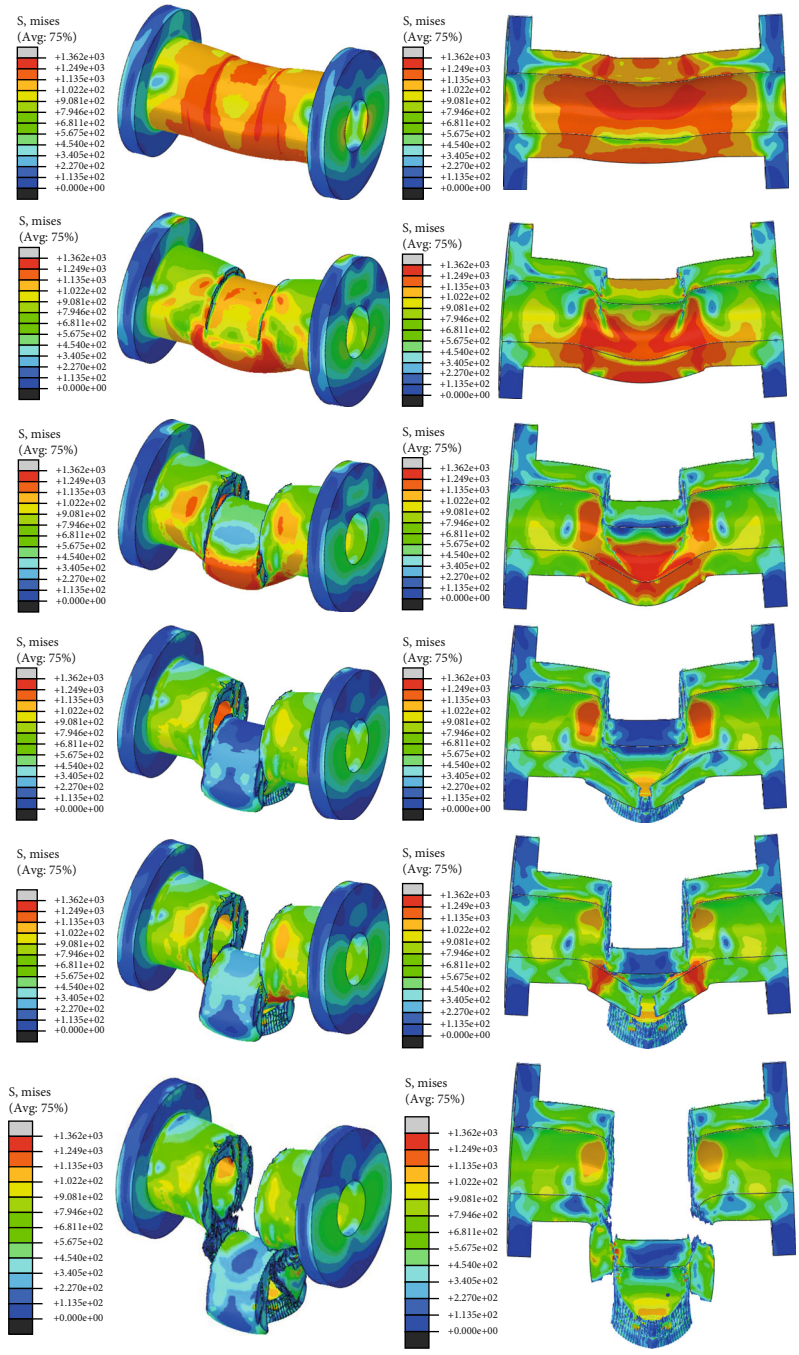

(d) Inner diameter of 28 mm

Figure 7: Fracture process of shear pins with different inner diameters.

mode of the shear pin. Therefore, the model validation of this research is effective. The time-history curves of the contact force between shear pins and its connecting lugs were illustrated as shown in Figure 6. It can be seen that the peak value of the contact force increases as the impact velocity increases. The variation tendency and incremental quantity are within expectations.

The model validation was meant to verify the failure mode change trend of pin structures with different inner/external diameter ratios, but not to generate the precisely same impact-loading responses. The comparison of the shear test results and the simulation results shows that the final failure mode of the shear pin with different inner/external diameter ratio can be predicted using the finite element model. Therefore, the model built in this research is used for further application.

3. Shear Fracture of Pins of Different Inner Diameters

The fracture process of shear pins with different inner diameters was simulated using the finite element model built in

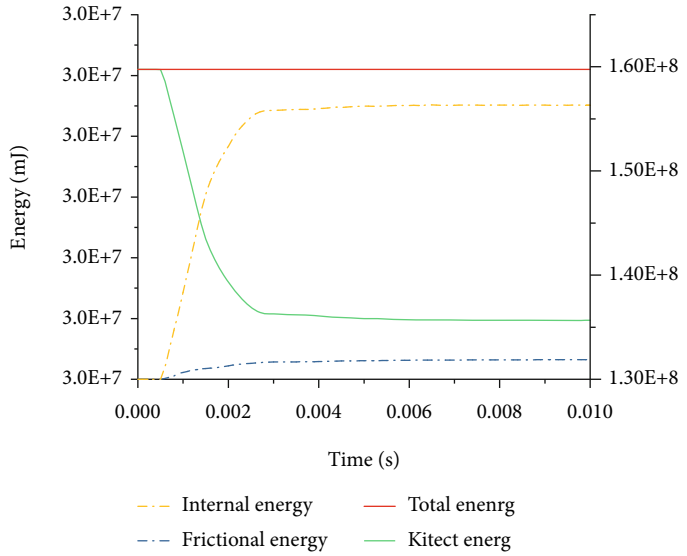

(a) Energy conversion of the clear failure mode

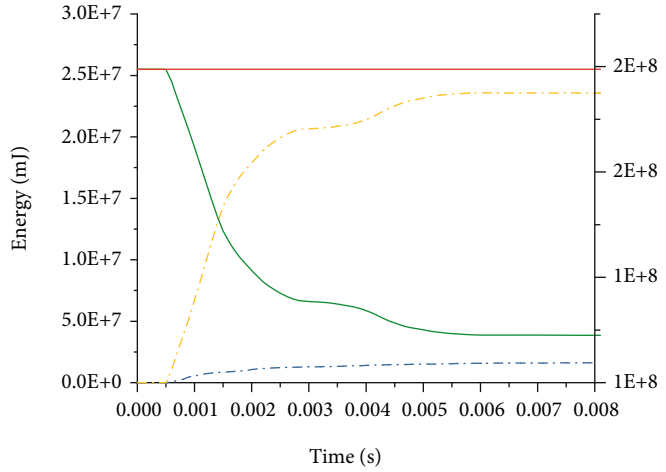

(b) Energy conversion of the complicated failure mode

Figure 8: Energy conversion of the shear pin in the fracture process.

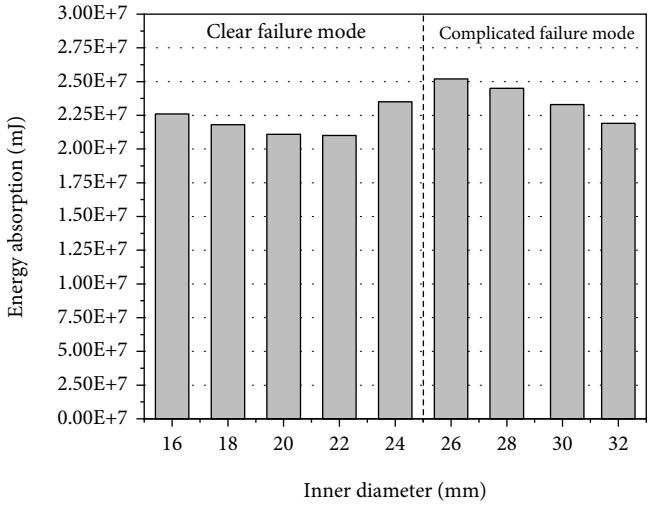

Figure 9: Energy dissipation of the shear pin with different inner diameters.

this research. The external diameter of the pin is 50 mm and the inner diameters of 16 mm, 18 mm, 20 mm, 22 mm, 24 mm, 26 mm, 28 mm, 30 mm, and 32 mm were selected to carry out simulations.

3.1. Structural Deformations. The structural deformations and stress distribution of the shear pin with different inner diameters are shown in Figure 7. The shear pins generate a clear failure mode and a complicated failure mode caused by the change of inner diameters.

When the inner diameter is less than or equal to 24 mm, the failure mode is clear and the fracture process has a short duration, as shown in Figures 7(a) and 7(b). Starting at the moment the shear pin was subjected to the impact load, the stress concentration occurred at pin surface. Then, the pin structure accumulated plastic strain and the stress concentration part of the pin structure firstly reached the limit of plastic strain and initiated damage accompanied with cracks. The crack extended downward along the cross

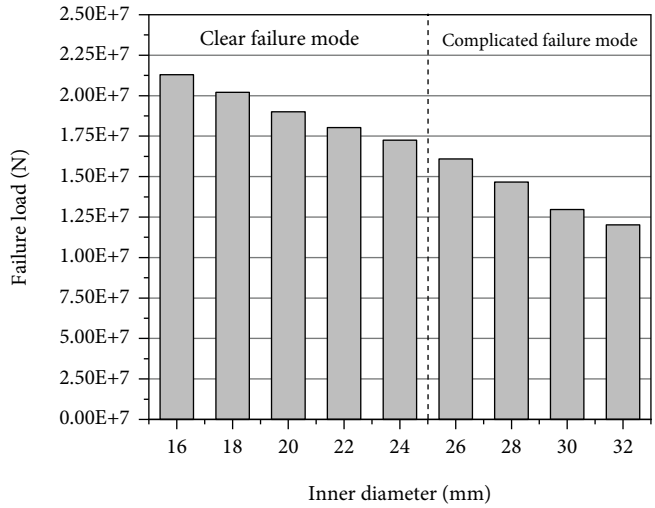

Figure 10: Failure load of shear pins with different inner diameters.

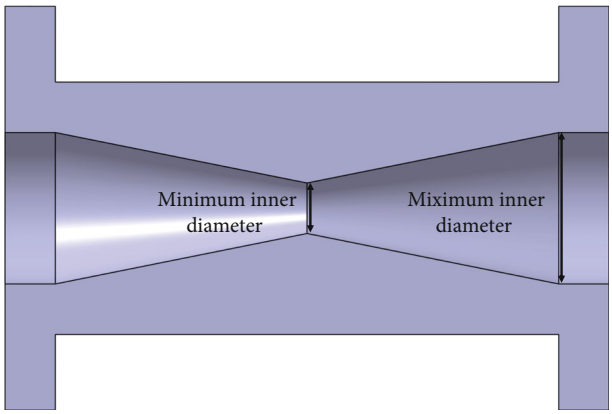

Figure 11: The new inner-varying configuration of the shear pin.

section of the pin structure. Meanwhile, the region where the lower part of pin structure intersects the double lugs also reached the limit of plastic deformation, and cracks extended upward. Finally, the crack on the upper and lower parts of the pin structure intersected, and the shear pin was completely broken into three sections.

When the inner diameter is more than or equal to 26 mm, the failure mode is more complicated and the duration of the fracture process is long. As shown in Figures 7(c) and 7(d), due to the decrease of the overall stiffness caused by the increase of the inner diameter, the pin structure had generated large deformations before the damage begins. The large deformation of the pin structure resulted in the change of crack propagation direction. When the crack originating from the upper part of the pin structure extended to the middle part of the shear pin, it began to expand along the inclined direction, then converged, and finally separated the upper part of the shear pin from the lower part. At this point, the pin structure had been broken into two pieces, while the lower part of the pin was still connected. Followed by the internal contact between the upper part and the lower part of the shear pin, the impact load was transmitted to the lower part and it finally resulted in the complete fracture of the pin structure.

The fracture process of the shear pin contains highly nonlinear structural damage and finite element simulation might have deviations; the changing trend of the failure modes is considered to be existed. In addition, the intervals between the lugs and shear pins have considerable contributions for the plastic deformations of the shear pins according to the simulations. Large intervals make the shear pins more prone to generate severe deformations in the fracture process. The above two kinds of failure modes greatly affect the structure separation process of shear pins. For the clear failure mode, the shear pin broke into three pieces quickly. In this case, the separation process can be completed smoothly without getting stuck. For the complicated failure mode, the fracture process is long lasting and involves internal contact of the pin structure, which would result in the difficulties in the structure separation process.

3.2. Energy Dissipation and Failure Load. A major issue in evaluation of impact behaviours of shear pins is energy dissipation. In the fracture process of shear pins, the initial kinetic energy and potential energy convert to internal energy and friction dissipation energy. The internal energy includes strain energy, plastic dissipation energy, and damage dissipation energy. The plastic dissipation energy contributes to over 90% of the internal energy while the damage dissipation energy accounts for less than 1% of the internal energy. The friction energy is caused by the contact between components and the self-contact of shear pins; it accounts for nearly 10% of the total energy dissipation.

Two energy conversion curves representing the fracture process of the two different failure modes are shown in Figure 8. The internal energy curve of the fracture process of the clear failure mode is smoother compared with that of the complicated failure mode. This is mainly because the fracture process of the complicated failure mode includes staged fracture and self-contact.

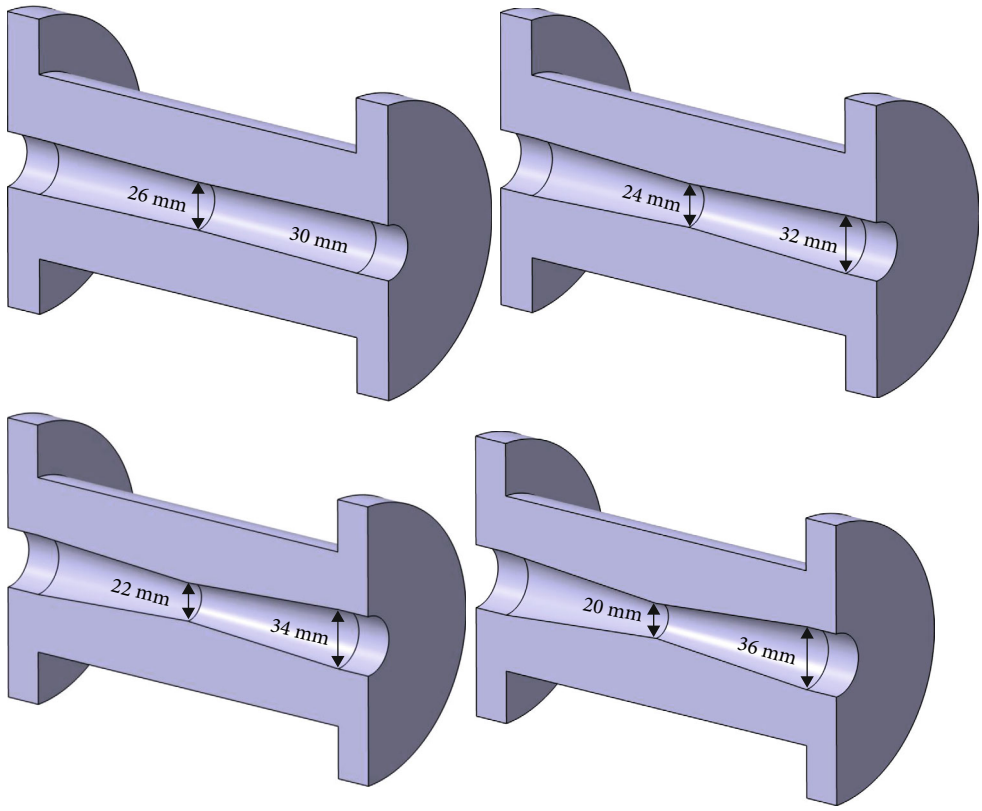

Figure 12: The new inner-varying configuration with different geometry parameters.

The total energy dissipated by shear pins with different inner diameters is demonstrated in Figure 9. As the inner diameter increases, the dissipated energy of shear pin in the fracture process decreases gradually. When the inner diameter increases to 26 mm, the failure mode of shear pin was converted from the clear failure mode to the complicated failure mode and the dissipated energy of the shear pin increases due to the large plastic deformation. After that, the dissipated energy of shear pin continues to decrease with the increase of inner diameter.

The failure load of the shear pin is used to determine the fracture load in the design of structure separation and is one of the most important parameters of the shear pin. Reasonable and accurate failure load is the key factor for accurate separation of structures. The fracture process of shear pin is a dynamic, time-varying, and nonlinear process. In this research, the contact force curve between the shear pin and its connecting lugs was extracted and the peak value was taken as the failure load. The failure load of shear pins with different inner diameters was compared as shown in Figure 10. It can be seen from the figure that the failure load of shear pins decreases as the inner diameter increases despite the change of failure modes.

4. Shear Fracture of Pins of Inner-Varying Configurations

4.1. Geometry and Parameters of the Inner-Varying Configuration. It has been illustrated in Section 3 that the failure load of the shear pin decreases as the inner diameter increases. Therefore, if the required separation load of the separation structure is small, the inner diameter should be promoted to reduce the failure load. However, as the inner diameter increases further, the failure mode of the shear pin changed and then large deformation and self-contact occurred in the fracture process, which would result in difficulties in the structural separation process. That is to say, it is difficult for the shear pin of the original configuration to have a clear failure mode while keeping low failure load. Another method to achieve both clear failure mode and low failure load is changing the external diameter of the shear pin and the intervals between the lugs. However, the external diameter and intervals of the lugs are related to the overall strength and stiffness of the connection structure and they are difficult to change. Therefore, a new configuration of shear pin without changing the external diameter was presented to improve the shear fracture performance as shown in Figure 11.

The new configuration of the shear pin has an inner diameter that decreases gradually from the middle to the two ends. The average inner diameter of shear pin of the new configuration was selected to be 28 mm to compare with the original shear pin whose inner diameter is 28 mm. The sum of the maximum inner diameter and minimum inner diameter equals to twice the average inner diameter. The value of maximum and minimum inner diameter will affect the internal shape of the shear pin, further changing the shear strength and failure mode in the fracture process.

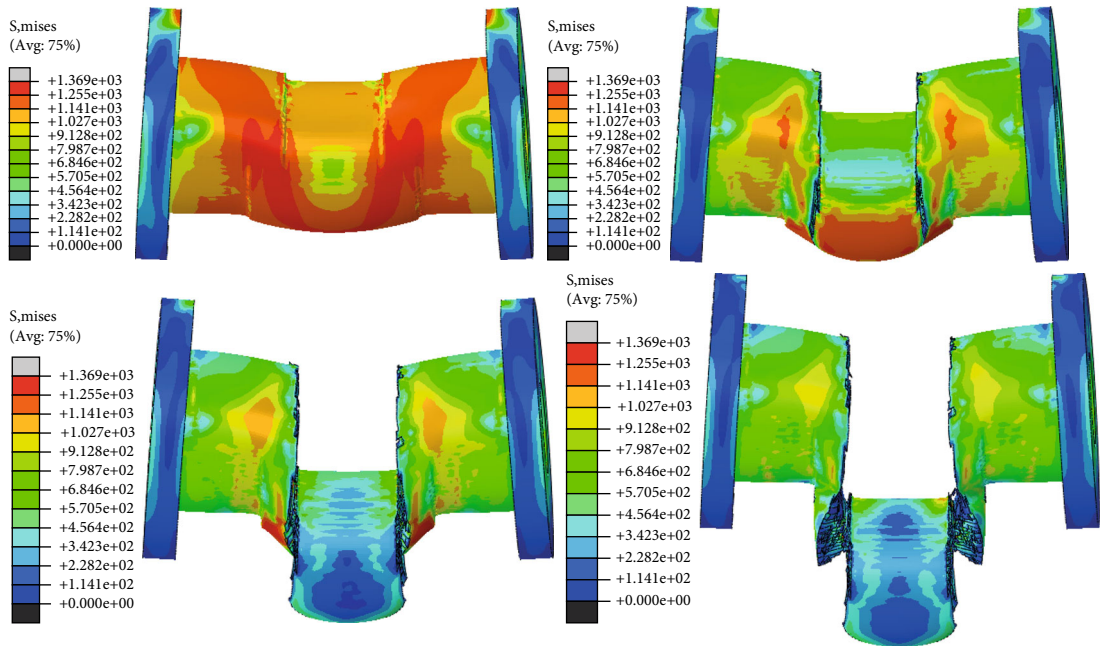

(a) Maximum inner diameter of 30 mm

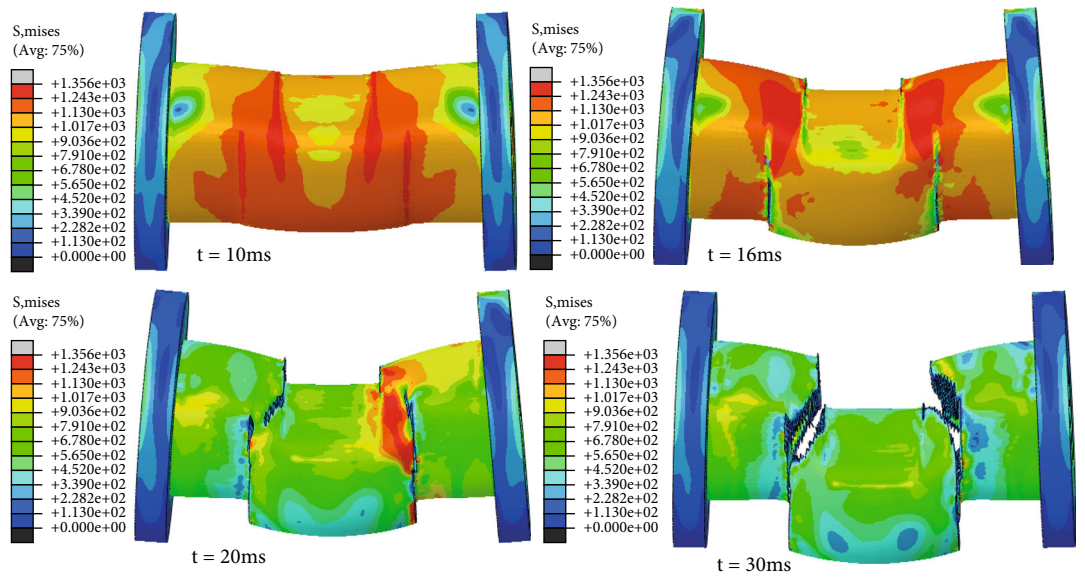

(b) Maximum inner diameter of 32 mm

Figure 13: Continued.

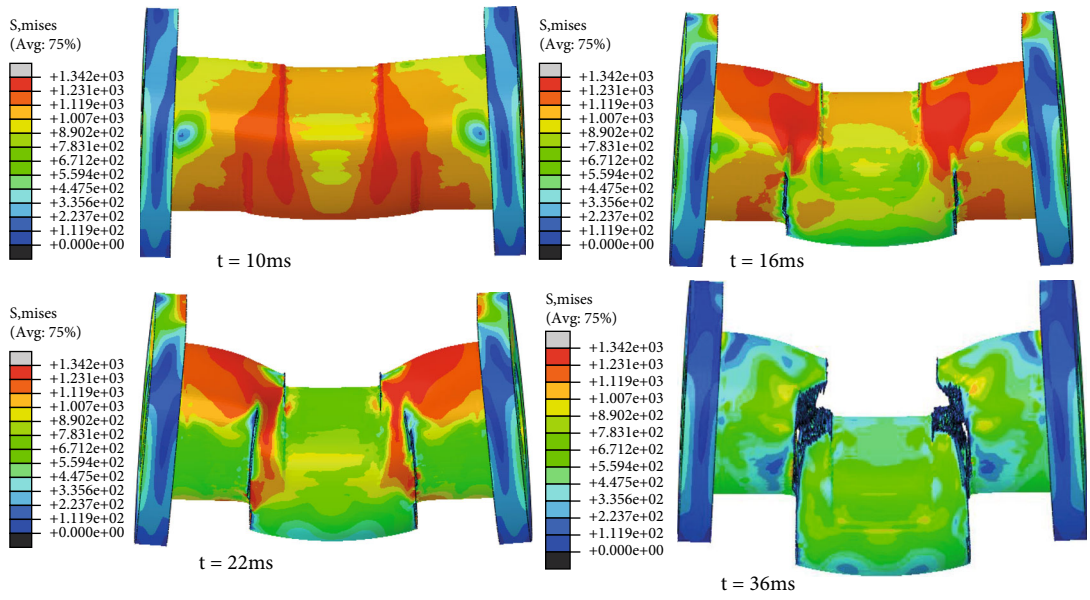

(c) Maximum inner diameter of 34 mm

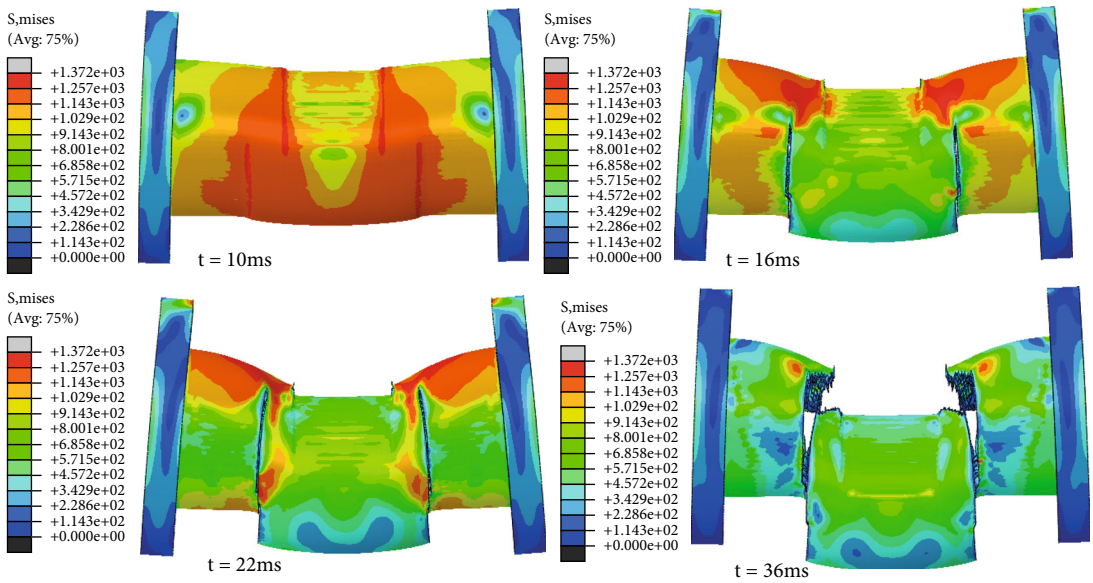

(d) Maximum inner diameter of 36 mm

Figure 13: Fracture process of shear pins with different inner diameters.

Therefore, the maximum inner diameters of 30 mm, 32 mm, 34 mm, and 36 mm were chosen to perform the fracture simulation of shear pins of the new configuration, as shown in Figure 12.

4.2. Structural Deformations. The structural deformations of shear pins of the new configuration with different maximum inner diameters are shown in Figure 13. For the shear pin with maximum inner diameter of 30 mm, the failure mode and the fracture process of shear pin of the new configuration are similar with the complicated failure mode. The crack originating from the upper part of the pin structure extended to the middle part and then began to expand along the inclined direction, finally resulting in large deformations and internal contact of the shear pin. For the shear pin with maximum inner diameter of 32 mm, 34 mm, and 36 mm, the region where the lower part of pin structure intersects the double lugs was reduced, which makes it easier for damage and crack to generate in the fracture process. It can be seen that the crack of the lower part of the shear pin occurred when the crack of the upper part extended upward, and then, the cracks intersected and the pin structure broke into three pieces. In this case, the clear failure mode was obtained.

Through the analysis and comparison of the structural deformations of the shear pin of the new configuration with different maximum inner diameters, it is found that the value of the maximum inner diameter changes the strength

Table 3: Energy dissipation and shear strength of shear pins of different configurations.

Shear pin configuration	New configuration (t/mm^3)				Original configuration (MPa)			
Inner diameter (mm)	Average inner diameter = 28				22	24	26	28
Maximum inner diameter (mm)	30	32	34	36				
Energy dissipation (10^7 mJ)	2.58	1.98	2.00	1.92	2.09	2.34	2.51	2.45
Shear strength (kN)	1511	1572	1600	1610	1796	1723	1605	1462
Failure mode	Second failure mode	First failure mode	First failure mode	First failure mode	First failure mode	First failure mode	Second failure mode	Second failure mode

distribution and affects the crack generation of the lower part of the shear pin. The crack generation is the key factor and has great influence on the failure mode of the fracture process.

4.3. Energy Dissipation and Failure Load. The total energy dissipation of the shear pin of the new configuration with different maximum inner diameters was demonstrated and compared with that of the original configuration, as shown in Table 3. For the shear pin with maximum inner diameter of 30 mm, the shear pin dissipated almost as much energy as the original configuration in the fracture process. This is because the failure mode is similar, and it contained large deformations. When the maximum inner diameter of the shear pin of the new configuration is higher than 30 mm, the total dissipated energy of the shear pin in the fracture process had an obvious decrease.

The failure load of the shear pin of the new configuration with different maximum inner diameters is also shown in Table 3. It is found that the increase of the maximum inner diameter of the shear pin resulted in the increase of the shear strength.

According to the discussion in Section 3, when the inner diameter increases to 26 mm, the failure load decreases to 1605 kN and the fracture of the shear pin was changed from the clear failure mode to the complicated failure mode. In other words, if the required failure load is equal or lower than 1605 kN, the shear pin of the original configuration would be unsuitable for the structural separation design that needs clear failure mode in the fracture process.

The shear pin of the new configuration with maximum inner diameter of 32 mm and 34 mm was 1572 kN and 1600 kN, respectively, which is lower than 1605 kN. But these shear pins all generate clear failure mode in the fracture. It means the shear pin of the new configuration is able to satisfy both the low failure load requirement and the clear failure mode in the fracture process.

5. Conclusion

This research mainly studies the fracture process of the hollow shear pin used in the separation structures through explicit finite element simulations. The shear fracture of shear pins with different inner diameters was simulated, and the following conclusions were drawn.

As the inner diameter increases, the fracture process of the shear pin changed from the clear failure mode to the complicated failure mode. The energy dissipation in the fracture process of the clear failure mode is generally lower than that of the complicated failure load due to the large plastic deformation in the fracture process. The failure load decreases with the increase of the inner diameter and is almost unaffected by the failure mode.

To solve the problem that the shear pin generates complicated failure mode when the inner diameter is large and the failure load is small, a new inner-varying configuration of shear pin without changing external shape of the pin structure was proposed. By simulating the shear fracture process of the new configuration and comparing with that of the original configuration, it is found that the new configuration is an effective design that can obtain both low failure load and clear failure mode.

Data Availability

The numerical data used to support the findings of this study are included within the article.

Conflicts of Interest

The authors declare that there is no conflict of interest regarding the publication of this paper.

References

[1] S. Sankar, M. Nataraj, and V. Raja, "Failure analysis of shear pins in wind turbine generator," *Engineering Failure Analysis*, vol. 18, no. 1, pp. 325–339, 2011.

[2] X. Gong, C. Xue, and J. Xu, "Dynamics simulation study on civil aircraft planned pavement emergency landing," *Journal of Vibroengineering*, vol. 17, no. 8, pp. 4496–4506, 2015.

[3] Y. Fang, C. Xue, and J. Xu, "Development of a load sensor for aircraft pylon interface load measurement," *Journal of Aircraft*, vol. 54, no. 1, pp. 336–345, 2017.

[4] K. Narayan, K. Behdinan, and P. Vanderpol, "An equivalent uniaxial fatigue stress model for analyzing landing gear fuse pins," *Strength of Materials*, vol. 38, no. 3, pp. 278–288, 2006.

[5] T. Kim, J. Shin, and S. Wook Lee, "Design and testing of a crashworthy landing gear," *ASME. ASME J. Risk Uncertainty Part B*, vol. 3, no. 4, Article ID 041006, 2017.

[6] *Crashworthy Landing Gear, SAE AIR 4566*, 1992.

[7] M. Zhang and W. Xu, "Study on fracture test of rocket shear pin," *Advanced Materials*, vol. 538-541, pp. 1579–1582, 2012.

[8] D. Cui, S. Yan, J. Li, Z. Qin, and X. Guo, "Dynamic analysis of satellite separation considering the flexibility of interface rings," *Proceedings of the Institution of Mechanical Engineers, Part G: Journal of Aerospace Engineering*, vol. 229, no. 10, pp. 1886–1902, 2015.

[9] T. Peng and N. Guo, "Experimental and numerical studies of shear pin fractures based, on linear and bilinear models," *Mechanika*, vol. 22, no. 4, pp. 245–250, 2016.

[10] T. Peng and N. Guo, "An equivalent linear model for shear pin fractures and its experimental verification," *Journal of Vibroengineering*, vol. 18, no. 8, pp. 5281–5290, 2016.

[11] N. Antoni, "A study of contact non-linearities in pin-loaded lugs: separation, clearance and frictional slipping effects," *International Journal of Non-Linear Mechanics*, vol. 58, pp. 258–282, 2014.

[12] X. Zhao, C. Fang, Y. Chen, and Y. Zhang, "Failure behaviour of radial spherical plain bearing (RSPB) joints for civil engineering applications," *Engineering Failure Analysis*, vol. 80, pp. 416–430, 2017.

[13] A. Strozzi, A. Baldini, and M. Nascimbeni, "Maximum equivalent stress in a pin-loaded lug subject to inclined loading," *The Journal of Strain Analysis for Engineering Design*, vol. 41, no. 4, pp. 297–309, 2006.

[14] R. Grant and B. Flipo, "Parametric study of the elastic stress distribution in pinloaded lugs modelled in two and three dimensions and loaded in tension," *The Journal of Strain Analysis for Engineering Design*, vol. 44, no. 6, pp. 473–489, 2009.

[15] H. Dong, *Static Analysis and Experimental Verification of Shear Strength of Aircraft Off Pin, [M.S. Thesis]*, Shenyang Ligong University, CHN, 2017.

[16] R. Zhang, X. Zhi, and F. Fan, "Plastic behavior of circular steel tubes subjected to low-velocity transverse impact," *International Journal of Impact Engineering*, vol. 114, pp. 1–19, 2018.

[17] F. Xu, X. Wan, and Y. Chen, "Design optimization of thin-walled circular tubular structures with graded thickness under later impact loading," *International Journal of Automotive Technology*, vol. 18, no. 3, pp. 439–449, 2017.

[18] M. Khedmati and M. Nazari, "A numerical investigation into strength and deformation characteristics of preloaded tubular members under lateral impact loads," *Marine Structures*, vol. 25, no. 1, pp. 33–57, 2012.

[19] A. Mondelin, F. Valiorgue, J. Rech, M. Coret, and E. Feulvarch, "Hybrid model for the prediction of residual stresses induced by 15-5PH steel turning," *International Journal of Mechanical Sciences*, vol. 58, no. 1, pp. 69–85, 2012.

[20] H. Zhen, X. Pu, and C. Zong, "Methodology of identification of Johnson-Cook constitutive parameters for cutting processes," *Journal of Plasticity Engineering*, vol. 23, pp. 197–201, 2016.

[21] P. Ponnusamy, S. H. Masood, D. Ruan, and S. Palanisamy, "Effect of build orientation and elevated temperature on microhardness and deformation of dynamically tested SLM processed AlSi12 alloy," *Materials Today: Proceedings*, vol. 38, pp. 2488–2492, 2021.

[22] D. Roberts, Y. Zhang, I. Charit, and J. Zhang, "A comparative study of microstructure and high-temperature mechanical properties of 15-5 PH stainless steel processed via additive manufacturing and traditional manufacturing," *Progress in Additive Manufacturing*, vol. 3, no. 3, pp. 183–190, 2018.

[23] Z. Li, H. Chen, and H. Liu, "Emergency break-away typical structure design and test of civil aircrafts," *Journal of Nanjing University of Aeronautics & Astronautics*, vol. 49, no. 1, pp. 87–93, 2017.